EXPERIMENTAL STUDY ON THE OPTIMIZATION OF AIR FLOW FOR INTAKE SYSTEMS

Beniuga Marius-Constantin[1,*], Tamașag Ioan[1,*]

[1]*Department of Mechanical Engineering, Stefan cel Mare University of Suceava, Romania*
13 University Street, 720229,
e.mail: ioan.tamasag@usm.ro, marius.beniuga@usv.ro.

Abstract: *The creation of the swirl effect is an important process for the operation of ICE (internal combustion engines) with gasoline or diesel, the phenomenon taking place between the intake manifold and the air filter. Precise mixture control is essential for optimizing the combustion process and consequently engine performance and efficiency. This paper presents an experimental study on the possibility of optimizing the air flow through the intake manifold by developing a new air flow turbocharging system by modifying the geometry of the inner surface of the air intake manifold in the engine, which induces a swirling motion in the air flow, creating a homogeneous mixture of the engine fluid.*

Keywords: *intake, flow meter, airflow, swirl.*

1. Introduction

Gas losses are related to the dimensions, architecture and condition of the interior surfaces of the air supply system. Thus, a first source of drag is the air filter, in the case of MAS engines, the existence of the diffuser which introduces a significant change in the flow cross-section and inlet flap, implicitly adds drag.

The air flow meter mounted immediately downstream of the air filter is part of the air intake circuit of the engine. Its purpose is to obtain information and calculate the parameters of the volume of air entering the intake manifold as a function of the position of the intake pedal, setting values for the ECU (Engine Control Unit) module.

Taking these aspects into account, the need arises to specify some parameters that characterize the optimization of cylinder filling with a fresh air-fuel mixture.

At first, this parameter is the mass of fresh charge retained in the cylinder, a value that does not allow both optimal filling and comparisons of gas exchange in different engines. The amplitude and frequency of the pressure waves in the intake manifold influence the filling coefficient, so certain engine speeds may favour cylinder filling (figure 1.a) and other speeds may disadvantage cylinder filling (Figure 1.b).

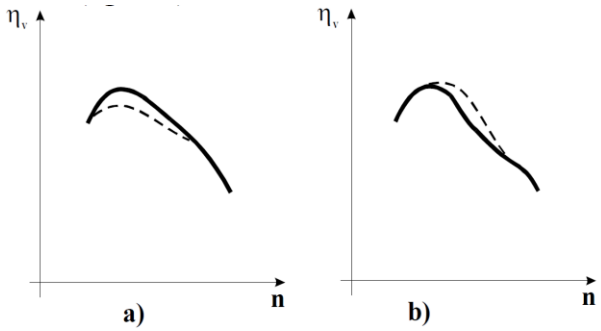

Figure 1. *Influence of pressure waves on the filling coefficient [1]*

For ICE engines, load variation is achieved by changing the amount of fuel injected into the cylinder, without any variable in the intake path. So, we can say that there is no direct connection between the filling efficiency and the load required to the engine, but we can explain an indirect connection between the mentioned factors, i.e. with the increase of the load the value of the thermal level of the engine increases, i.e. the fresh fluid absorbed in the engine increases with the decrease of the filling coefficient.

Therefore, in compression ignition internal combustion engines, the value of the filling efficiency is inversely proportional to the value of the load.

The aim of the present work is to create the swirl effect by redesigning the inner surface of the air flow meter body. For this purpose, a number of common methods of scanning reverse engineering [3, 4, 5] and additive manufacturing [6, 7] will be used.

2. Intake manifold construction concerned

2.1 Creating the 3D model on the inner surface

Figure 2: *Design of the air flow meter.*

The model was created by applying a reverse engineering method. In the first step, the original part (Figure 2), was scanned using a Nikon MCAx polyarticulated arm (Figure 3.a). Subsequently, using the reverse engineering software Geomagic Design X, the 3D shape of the part was constructed on the basis of the point cloud obtained from the scan (figure 3.b).

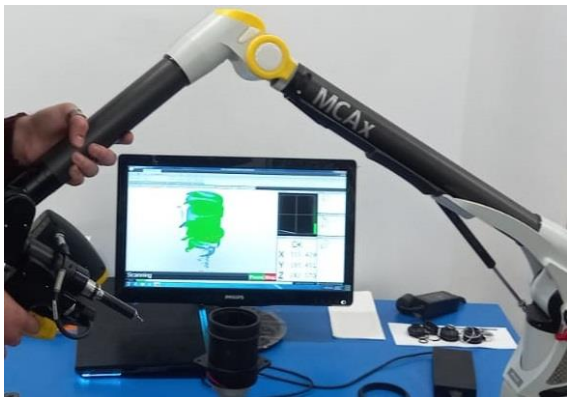

a.

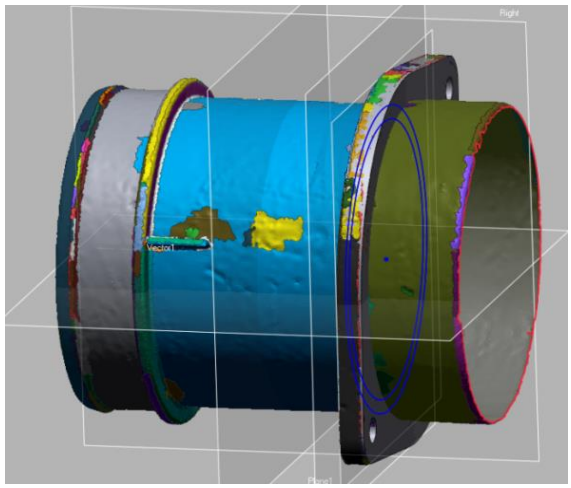

b.

Figure 3: *3D shape scanning and design by reverse engineering.*

After creating the 3D model of the original part, the swirl was ensured by redesigning the interior of the tubing. Thus, using Autodesk Inventor design software, the new 3D model shown in figure 4 was created.

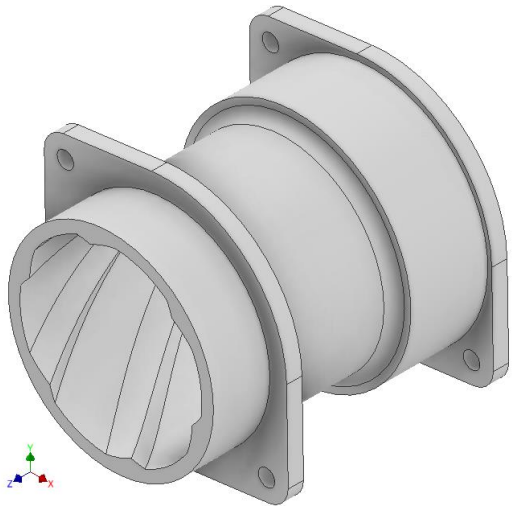

Figure 4: *Tubing redesign, isometric view.*

Figure 5 graphically illustrates the methodology for creating turbidities. On the inner surface of the cylindrical body, a series of elements were created for turbulence of the air sucked from the air filter housing area to the air collector.

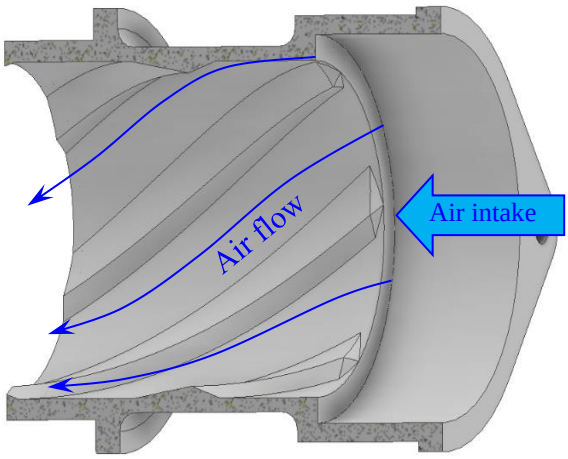

Figure 5: *Representation of air flow, sectional view.*

2.2. Manufacture of the inlet manifold

After creation of the 3D model, the part was practically manufactured by the Fused Deposition Modelling (FDM) additive manufacturing method, using FLSUN SuperRacer equipment (Figure 6).

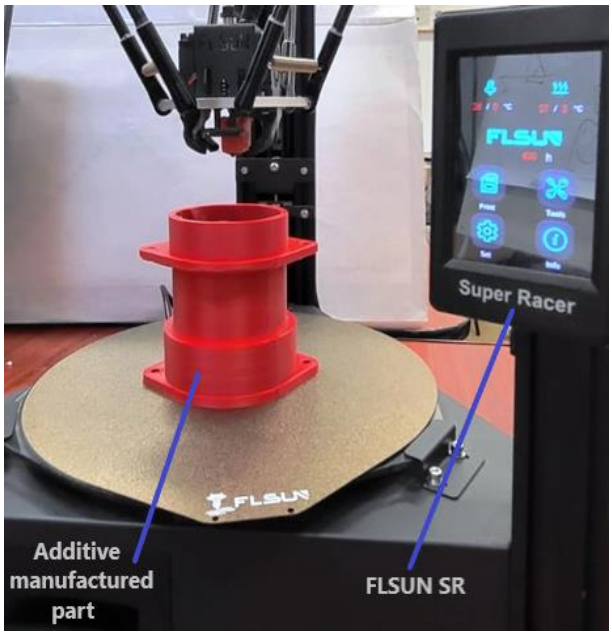

Figure 6: *Manufacture of the part.*

Figure 7: *Partial assembly of the final part.*

The material used for the manufacture was an acrylonitrile butadiene styrene (ABS) polymer, often used in the manufacture of plastic components for the automotive manufacturing industry.

Creating turbulence in channels with a cylindrical cross-section is an important issue in fluid engineering, as turbulence can improve heat transfer and fluid homogenization. Turbulence in a circular channel can be generated in various ways using flaps.

Flaps (fins) are elements designed to optimize homogenization and heat transfer (figure 7). They are structures or protrusions mounted on the surface of an object, such as a solid body or a fluid conducting surface, to modify the characteristics of the fluid flow or to fulfil specific purposes.

They are used in various applications, including aerodynamic and hydrodynamic engineering, to influence and control the direction and characteristics of fluid flow.

3. Experimental results

3.1 Operating parameters according to air flow meter (standard equipment)

Figure 8 shows the intake air flow variation curves as a function of the intake valve position and the air flow values stored in the ECU (Engine Control Unit) value map. The graph shapes were obtained by changing the intake valve position by repeatedly pressing the accelerator pedal (four times within 11 seconds, as shown in figure 8.a.

The data shown in the following images are obtained with a Delphi DS150E multi-marque automotive test and diagnostic device.

This study is performed for supercharged internal combustion engines with cylinder capacities between 2000[cm^2] and 3000[cm^2], but can also be used for naturally aspirated internal combustion engines, both SIE (spark ignition engines) and CIE (compression ignition engines).

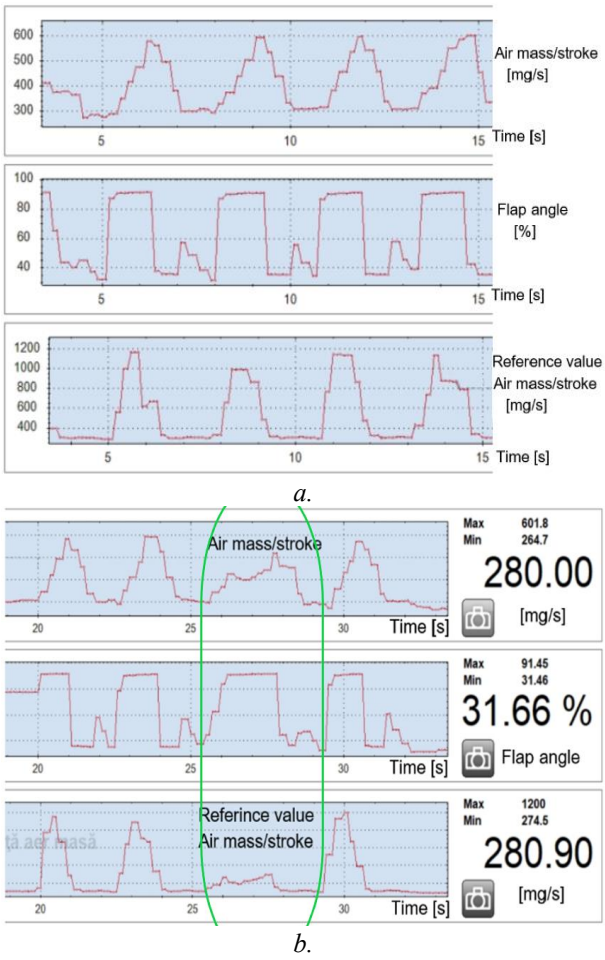

Figure 8: *Air mass flow variation curves obtained without changes in the inlet path [2].*

Figure 8.b shows the results of a similar number of four repeated throttle pedal actuations with the difference that the third engine speed increase is still in the 80% throttle opening range, but at a lower pedal actuation speed (according to the curves in Figure 8.b over a range of two seconds, compared to the curves in Figure 8.a where the third air throttle opening was over a range of one second).

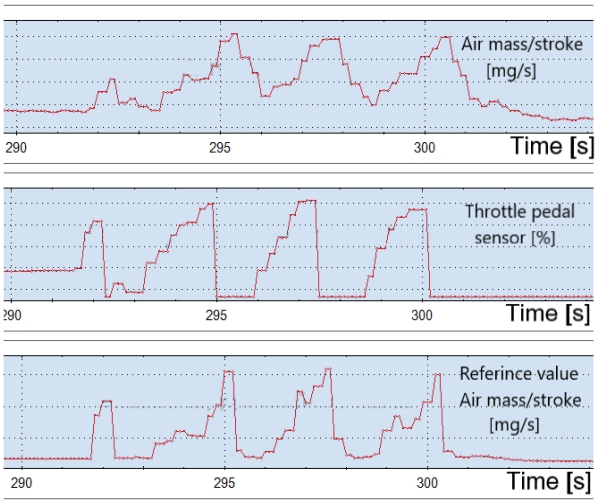

Figure 9: *Correlation of air channels with PWM values from throttle position sensor [8].*

The variation of the engine air mass flow rate as a function of the throttle pedal position (PWM) is shown in Figure 9, where there is a very precise correlation between the throttle open and closed position and the PWM signal from the throttle pedal electronic control module.

Subsequent to the graphical data acquisition presented above, cumulative tabulated data were also extracted as shown in Figures 10 and 11. For this purpose, four speed steps were established for the engine operation during the experiment as follows:

I - 700[rpm], idle speed, effective 701[rpm] as shown in figure 10.a;

II - 1000[rpm], effective 977[rpm] as shown in figure 10.b;

III - 1500[rpm], effective 1515[rpm] as per figure 10.c;

IV - 2000[rpm], effective 1984[rpm] according to figure 10.d.

Name	Value	Unit
Accelerator pedal sensor, PWM	8.26	%
Air inlet temperature sensor	31.16	°C
Air mass	23.90	kg/h
Air mass reference value	228.40	mg/s
Air mass/stroke	227.50	mg/s
Atmospheric pressure	952	hPa
Coolant temperature	59.86	°C
Engine speed	701	Rpm

a.

Name	Value	Unit
Accelerator pedal sensor, PWM	13.88	%
Air inlet temperature sensor	31.96	°C
Air mass	36.70	kg/h
Air mass reference value	249.00	mg/s
Air mass/stroke	249.20	mg/s
Atmospheric pressure	952	hPa
Coolant temperature	61.96	°C
Engine speed	977	Rpm

b.

Name	Value	Unit
Accelerator pedal sensor, PWM	17.18	%
Air inlet temperature sensor	32.06	°C
Air mass	60.00	kg/h
Air mass reference value	264.50	mg/s
Air mass/stroke	268.00	mg/s
Atmospheric pressure	952	hPa
Coolant temperature	62.26	°C
Engine speed	1515	Rpm

c.

Name	Value	Unit
Accelerator pedal sensor, PWM	19.93	%
Air inlet temperature sensor	33.56	°C
Air mass	89.60	kg/h
Air mass reference value	290.80	mg/s
Air mass/stroke	295.60	mg/s
Atmospheric pressure	952	hPa
Coolant temperature	65.86	°C
Engine speed	1984	Rpm

d.

Figure 10: *Tabulated parameters (standard equipment).*

3.2. Operating parameters according to the air flow meter equipped with the manufactured element

For this purpose, four speed steps were also established for engine operation during the experiment, as follows:

I - 700[rpm], idle speed, effective 701[rpm] according to figure 11.a;

II - 1000[rpm], effective 1007[rpm] as shown in figure 11.b;

III - 1500[rpm], effective 1502[rpm] as per figure 11.c;

IV - 2000[rpm], effective 2002[rpm] according to figure 11.d.

Name	Value	Unit
Accelerator pedal sensor, PWM	8.26	%
Air inlet temperature sensor	33.86	°C
Air mass	24.70	kg/h
Air mass reference value	236.70	mg/s
Air mass/stroke	236.10	mg/s
Atmospheric pressure	952	hPa
Coolant temperature	59.36	°C
Engine speed	700	Rpm

a.

Name	Value	Unit
Accelerator pedal sensor, PWM	14.20	%
Air inlet temperature sensor	34.16	°C
Air mass	38.80	kg/h
Air mass reference value	258.20	mg/s
Air mass/stroke	258.10	mg/s
Atmospheric pressure	952	hPa
Coolant temperature	59.66	°C
Engine speed	1007	Rpm

b.

Name	Value	Unit
Accelerator pedal sensor, PWM	17.01	%
Air inlet temperature sensor	36.06	°C
Air mass	62.70	kg/h
Air mass reference value	279.00	mg/s
Air mass/stroke	277.50	mg/s
Atmospheric pressure	952	hPa
Coolant temperature	63.86	°C
Engine speed	1502	Rpm

c.

Name	Value	Unit
Accelerator pedal sensor, PWM	20.41	%
Air inlet temperature sensor	37.36	°C
Air mass	97.20	kg/h
Air mass reference value	320.60	mg/s
Air mass/stroke	322.30	mg/s
Atmospheric pressure	952	hPa
Coolant temperature	65.26	°C
Engine speed	2002	Rpm

d.

Figure 11: *Tabulated parameters (fitting with manufactured item).*

4. Conclusions:

By processing the experimental data, the following results were quantified, noting that for both test variants, four engine speeds were established for the necessary data acquisition. These engine speeds are 700 rpm (for the idle mode), 1000 rpm, 1500 rpm and 2000 rpm at a temperature regime of 60°C to 64°C (not at nominal operating temperature because the tests were performed with the vehicle stationary), and the important and highly accurate parameters are:

- Throttle pedal position [%];
- Intake air mass flow rate [mg/s], for each operating cycle measured;
- Reference intake air mass flow rate [mg/s], for each duty cycle, provided by the ECU value map;
- Engine speed [rpm].

From this data it was concluded that when using the built element, an increase of only 3.6% was obtained for idle speed, followed by the same value for 1000 rpm, then 5.4% for 1500 rpm and 8.4% for 2000 rpm. It can be seen that with increasing engine running speed, we obtain an increase in the value of the air mass flow rate for each running cycle.

If an average percentage value of the continuous difference is desired, it has been calculated at the value of 5.25%.

Figure 12: *The intake pipe in the composition of the test system*
(equipment with manufactured item).

References

1. [Grunwald, 1980] Grunwald B., *Teoria, calculul si constructia motoarelor pentru autovehicule rutiere*, Ed. Didactica si Pedagogica, Bucuresti, 1980.
2. [Burnete, 2021] Burnete N.V, Burnete N, *Motoare cu ardere internă și Termodinamică*, Noțiuni fundamentale, U.T.PRESS, Cluj-Napoca, 2021.
3. [Dúbravcík, 2012] Michal Dúbravcík, Štefan Kender, *Application of reverse engineering techniques in mechanics system services*, Procedia Engineering 48, pp. 96 – 104, doi: 10.1016/j.proeng.2012.09.491, 2012.
4. [Eslami, 2017] Eslami, A. M., *Integrating Reverse Engineering and 3D Printing for the Manufacturing Process*, ASEE Annual Conference & Exposition, Columbus, Ohio. 10.18260/1-2—28558, 2017.
5. [Robin, 2021] Robin H. Helle, Hirpa G. Lemu, *A case study on use of 3D scanning for reverse engineering and quality control*, Materials Today: Proceedings, Vol. 45(6), pp. 5255-5262, doi.org/10.1016/j.matpr.2021.01.828, 2021.
6. [Anifantis, Findik, 2012] Anifantis N, Findik F, *A Review of Additive Manufacturing*, Volume Article ID 208760, doi.org/10.5402/208760, 2012.
7. [Frazier, 2014] Frazier, W.E., *Metal Additive Manufacturing: A Review*. J. of Materi Eng and Perform 23, 1917–1928. doi.org/10.1007/s11665-014-0958-z, 2014.
8. Dispozitiv de testare electronic multimarcă Delphi DS150E.